Global Quantum Leap International Research and Training Experience Final Report

2023 GQL IRTE Intern: Jake Markowski
2023 GQL IRTE Intern Affiliation: Department of Physics and Astronomy, University of Rochester

2023 GQL IRTE Principal Investigator: Dr. Christoph Stampfer
2023 GQL IRTE Program Location: RWTH Aachen, Aachen, Nordrhein-Westphalia, Germany

Contact: j.markowski@rochester.edu, stampfer@physik.rwth-aachen.de

Website: https://www.globalquantumleap.org/

Abstract:

Bilayer graphene (BLG) has a highly tunable band gap which suggests the material may eventually be used as a medium for spin-valley qubits similar to those already developed in silicon. Once these qubits are actualized, many of the results of traditional semiconductor qubits may be recreated, and perhaps expanded upon due to BLG's valley pseudo-spin which has a g-factor an order of magnitude larger than the spin g-factor. In this report we provide an introduction to BLG quantum dots and present details of Hamiltonians developed to better understand the one and two particle states within a bilayer graphene quantum dot array. These models may be used to explain the finite bias spectroscopy measurements from the detuning cut across the (1,1) to (0,2) transition and to design future experiments.

Introduction

Bilayer graphene (BLG) has been the subject of intense study in recent years due to its unique band structure, high carrier mobility, and potential to host high-coherence spin and valley qubits. The material has received particular interest within the field of quantum information because its low hyperfine and spin-orbit coupling provide an information retention advantage when compared to traditional semiconductor-based qubits. Bilayer graphene possesses a unique band structure in which the conduction and valence bands meet with a linear dispersion relation at six Dirac cones - this is shown in figure (1). Critically, a band gap (approximately 25 meV) may be introduced and finely tuned using a perpendicular displacement field [2]. Once the band gap is established, the material will behave as a semiconductor. As such, we can confine individual electrons or electron-holes in gate-defined quantum dots (QDs). Due to the symmetry of the Dirac cones, a single BLG QD may be tuned to host precise numbers of electrons *or* holes, as shown in figure (3) [2]. Since BLG devices may operate nearly identically with electrons or holes, for the duration of this report we will avoid any unnecessary distinctions by referring to electrons and holes as particles.

Theoretical investigations have suggested universal quantum gates can be achieved by manipulating spin and valley qubits within a pair of quantum dots [10]. Recent experimental works have shown the promise of such a method in silicon-based qubits [3, 4]. It is worthwhile to further develop BLG QDs with the objective of creating spin-valley qubits which utilize the material's notable valley splitting and low noise properties. A necessary step in this progress is to comprehensively understand the two-particle states accessible in a BLG double quantum dot (DQD) array. This report will provide an overview of the Hamiltonian matrices developed to describe the energetic spectrum of BLG DQDs.

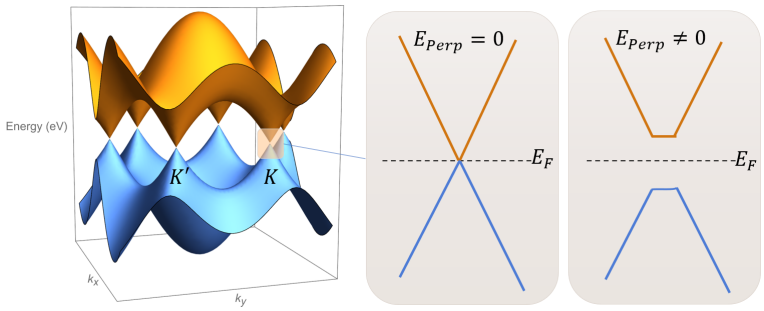

Figure 1: **Left:** the hexagonal band structure of bilayer graphene with two non-equivalent Dirac cones marked. **Right:** A rough example of how a band gap may be induced and tuned via a displacement field applied perpendicular to the BLG lattice.

Quantum Dots

In this section, we provide a brief overview of BLG QD devices and their fabrication. Constructing nano-scale devices with 2D materials provides a few additional challenges in comparison to semiconductor-based devices. The process starts with the mechanical exfoliation of sheets of graphite, hexagonal boron nitride (hBN), and bilayer graphene. The sheets are then physically stacked to form a heterostructure in the order, graphite, hBN, BLG, hBN, graphite. It should be noted that the strain introduced during exfoliation and stacking causes some variability in the performance of the devices, specifically in what the valley g-factor is. Since hBN is an insulating material, this heterostructure will provide the first degree of confinement in the z-direction. Moreover, the voltages applied to the SG and graphite back gate produce the displacement field which creates the band gap. Next, a layer of gold will be deposited, forming a split gate (SG) which further confines the active region to a 1D channel. The following step is to etch through the graphite and hBN to form Ohmic contacts on each end of the channel: applying voltages to each end allows for a bias voltage to be formed between the source and drain. From here, the fabrication is quite similar to that of semiconductor quantum dot devices; e-beam lithography and atomic layer deposition are used to develop a series of electrically-separated finger and plunger gates which can be tuned to provide the final degree of confinement. These final gates may be used to adjust the tunnel coupling between the two dots and the depth of the energy well. We may introduce a transition from the regime where both dots contain one particle to one where they are both in the right dot, i.e. $(1,1) \rightarrow (0,2)$ by adjusting the detuning, ϵ, which is difference in the potential well depth between the dots.

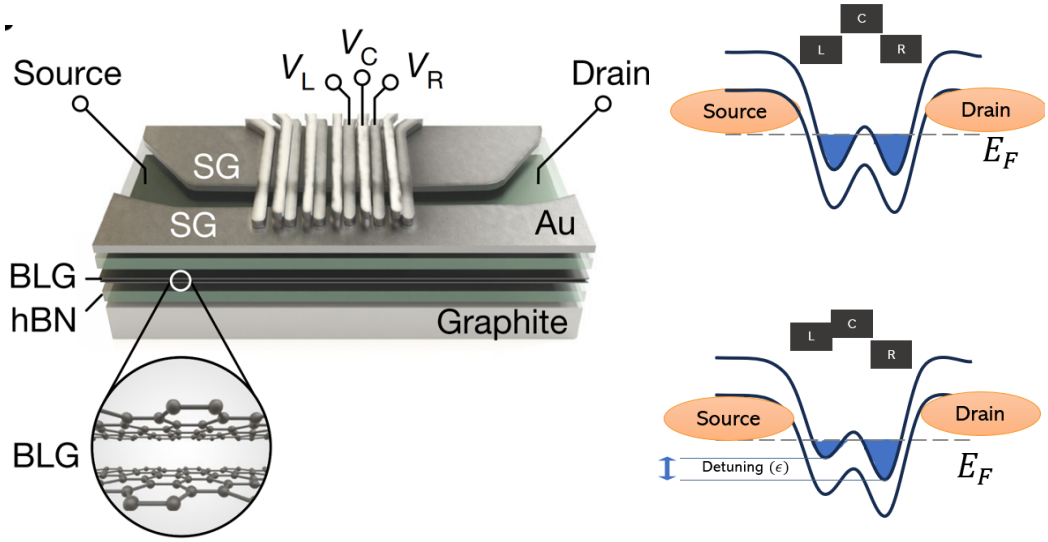

Figure 2: **Left:** Representative diagram of BLG DQD device with hBN-BLG-hBN-Graphite Van-Der-Waals heterostructure. The gate structure necessary to define and control QDs is also shown. Image taken from [1]. **Right:** Example of detuning DQD from (1,1) to (0,2) states using the left and right finger gates.

Hamiltonians and Energy Spectrum

Allowed States

Each electron or hole in BLG must possess a spin state ($|\uparrow\rangle$ or $|\downarrow\rangle$) and a valley pseudo-spin dependent on which Dirac cone it is occupying: $|+\rangle$ if in the K' valley or $|-\rangle$ when in the K valley. The valley pseudo-spin has a magnetic moment with a g-factor between 5 and 20 times

larger than the spin g-factor of two. The valley magnetic moment is related to Berry curvature and is an effect caused by the topological nature of the material. It should be noted that the sign of the magnetic moment is flipped for different valleys and for electrons/holes, as shown in figure (3). Thus, a single particle in an orbital ground state may be in a superposition of up to four states: $|+\uparrow\rangle$, $|+\downarrow\rangle$, $|-\uparrow\rangle$, and $|-\downarrow\rangle$.

With two possibilities both the spin and valley state of each particle, it follows that there are sixteen composite states available to a two particle system in a BLG QD. Just as it is necessary to describe the spin state of two electrons in a singlet/triplet basis, we must do the same for the valley states. This means that each state must be represented as a singlet or triplet for its spin and valley state. To be precise, the spin and valley states of a two particle configuration should be represented by elements of

$$\{|S^s\rangle, |T_0^s\rangle, |T_+^s\rangle, |T_-^s\rangle\} \otimes \{|S^v\rangle, |T_0^v\rangle, |T_+^v\rangle, |T_-^v\rangle\}.$$

As an example, the state $|T_-^s T_-^v\rangle = |-- \downarrow\downarrow\rangle$ will be the lowest energy state when a sufficiently strong out-of-plane magnetic field, $B_\perp$, is applied. A somewhat more interesting example is the spin-singlet, valley neutral triplet, $|S^s T_0^v\rangle = \frac{1}{2}\left(|+- \uparrow\downarrow\rangle - |+- \downarrow\uparrow\rangle + |-+ \uparrow\downarrow\rangle - |-+ \downarrow\uparrow\rangle\right)$. Singlet states are anti-symmetric under exchange whereas triplet states are all symmetric. Since electrons and electron holes are fermions, their composite wavefunction must by anti-symmetric under particle exchange. Thus, if we have a state which is either a double triplet or double singlet, it must be in an orbitally anti-symmetric state in which one particle is in the ground state while the other is in the excited state. If the spin-valley component of the wavefunction is anti-symmetric (i.e. it is composed of a singlet and a triplet state), the orbital state must be symmetric - meaning both particles are in their lowest orbital state.

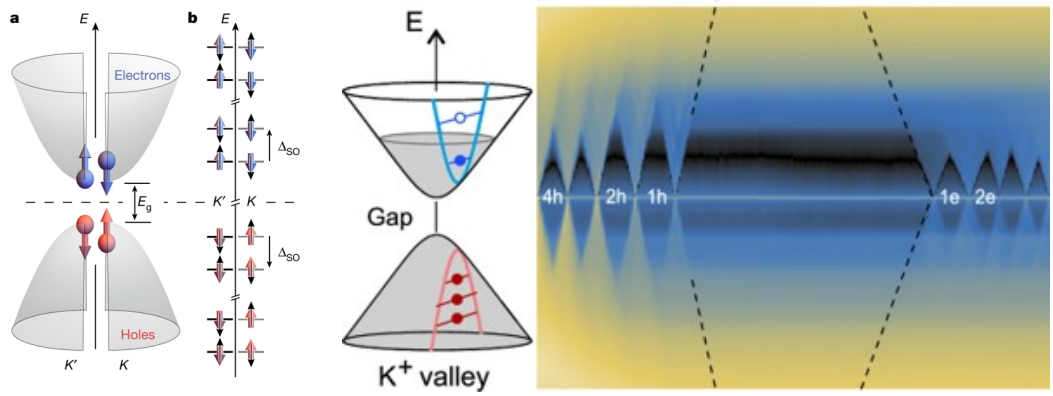

Figure 3: **Left:** Illustration of the spin and valley states present in the K' and K valleys. **Middle:** Example of single-electron QD. The Fermi level within the dot is set such that all the holes are filled an only one electron may exist in the conduction band. **Right:** Key result from Banszerus et. al. displaying the Coulomb diamonds for a BLG QD device which can be tuned to support electrons or holes [2]. *Images from* [1,2].

Diagonal Hamiltonian Elements

The diagonal elements of the Hamiltonian matrices are already well understood and have been well explained by Knothe et. al. [6,7]. As these have the largest impact on the energy spectrum, we will briefly list them here.

- *$B_\perp$ Zeeman Splitting:* When a magnetic field perpendicular to the BLG flake ($B_\perp$) is applied, the spin and valley magnetic moments will couple with the field, resulting in significant Zeeman spitting $\left(H_{\text{Zeeman}} = \frac{1}{2}\mu_B B_\perp(g_s\sigma + g_v\tau)\right)$, where μ_B is the Bohr magneton, The spin

g-factor, $g_s = 2$, is generally one order of magnitude less than the valley g-factor g_v which is dependent on the geometry of the dot and wavefunction. In the above expression, σ and τ represent the spin and valley states respectively and are equal to $+1$ for spin up/the $+$ valley and -1 for spin down/the $-$ valley.

- *Kane-Mele Spin-Orbit Coupling:* The spin and valley magnetic moments will couple with one another, resulting in Kramer's pairs [5]. States with aligned magnetic moments $\left(|+\uparrow\rangle, |-\downarrow\rangle\right)$ will have an energy $2\Delta_{SO}$ less than the antialigned magnetic moments $\left(|+\downarrow\rangle, |-\uparrow\rangle\right)$.
- *Orbital Splitting:* Particles in the first excited state will have an energy of Δ_{Orb} greater than their counterpart in the ground state. This work only considers states with at most one particle in the excited state.
- *Lattice Scale Interactions:* When there are two particles in the ground-state or a single quantum dot, short-range symmetry breaking interactions become relevant. With our model, this only applies to the orbitally symmetric $(0, 2)$ states. The energy differences can be experimentally mapped to δ_1 and δ_2 constants [6, 8].

Non-diagonal Hamiltonian Elements

- $B_\parallel$ *Zeeman Splitting:* Since the valley pseudo-spin exists only in the out of plane direction, it does not couple to in-plane magnetic fields. Thus the in-plane Zeeman splitting is dependent only on the spin state. Such a field will result in hybridization of states written with an up-down basis relative to the lattice.
- *'Flip' Coupling* The core of my project was in developing a model for coupling that exists when there is a mechanism which allows the particle to change spin and/or valley states. Specifically we consider spin coupling (Δ_S), valley coupling (Δ_V) and spin-valley coupling (Δ_{SV}). In quantum mechanics, inter-state coupling like this results in avoided crossings in which the energy eigenvalues will become hybridized between the two states, but never equal. Many qubit operations are based on Landau-Zener-Stückelburg transitions which are diabatic transitions between states at an avoided crossing [9].

Single Particle Hamiltonian

While the Hamiltonian for a single particle in a BLG QD is already well understood [6, 8], it is worthwhile to discuss it here as a means of gaining insight on the available states and their energies. We will focus primarily on the single particle spectrum, because the two-particle Hamiltonians developed over the course of this research cannot fit on a single page and are too complex for the context of this report. The Hamiltonian for a single confined BLG particle in the basis of $\{|+\uparrow\rangle, |+\downarrow\rangle, |-\uparrow\rangle, |-\downarrow\rangle\}$ is

$$H_1 = \begin{pmatrix} \frac{1}{2}(B_z\mu_B(g_s+g_v)+\frac{\Delta SO}{2} & -i\Delta S+\frac{1}{2}B_x g_s\mu_B & \Delta V & -i\Delta SV \\ i\Delta S+\frac{1}{2}B_x g_s\mu_B & \frac{1}{2}B_z\mu_B(-g_s+g_v)-\frac{\Delta SO}{2} & i\Delta SV & \Delta V \\ \Delta V & -i\Delta SV & \frac{1}{2}B_z\mu_B(g_s-g_v)-\frac{\Delta SO}{2} & -i\Delta S+\frac{1}{2}B_x g_s\mu_B \\ i\Delta SV & \Delta V & i\Delta S+\frac{1}{2}B_x g_s\mu_B & \frac{1}{2}B_z\mu_B(-g_v-g_s)+\frac{\Delta SO}{2} \end{pmatrix}.$$

Here you can see the $B_\perp$ Zeeman splitting and Kane-Mele spin orbit coupling along the diagonal with flip coupling and $B_\parallel$ Zeeman splitting filling the rest of the Hamiltonian. In figure (4), we plot the eigenvalues of the above Hamiltonian with respect to $B_\perp$ and $B_\parallel$.

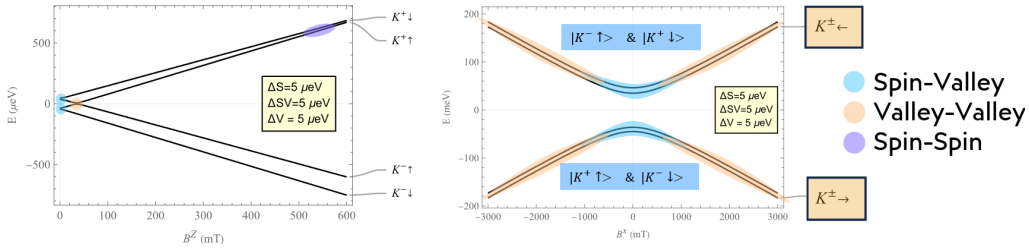

Figure 4: **Left:** Result of plotting H_1 with respect to $B_\perp$. The short-range flip coupling is only active at $B_\perp = 0mT$ (spin-valley coupling), $B_\perp = 20mT$ (valley coupling) and $B_\perp = 550mT$ (spin coupling). **Right:** Result of plotting $B_\parallel$ over a range of 3 T. Despite a much larger magnetic field, the Zeeman splitting is far less than in the left plot due to the fact the valley magnetic moment does not couple with an in-plane magnetic field. In this plot, you can see that at zero magnetic field the states are naturally in a spin up/down basis, but at higher fields they are shifted toward a right/left basis.

Hamiltonian for two Particles in a Single dot

As previously mentioned, it is not worthwhile for the context of this report to properly describe the Hamiltonian and spectrum for the two particle states. We will simply present the result of plotting the diagonal elements and the eigenvalues of the full Hamiltonian in figure (5). The left portion of the figure closely mirrors a key result of Möller et. al. [8]; details of this energy spectrum are carefully explained and matched to experiment in that work. Details of the (0,2) Hamiltonian are available upon request.

With figure (5), one may see that the bulk structure of the energy levels is a result of the diagonal Hamiltonian elements. But that is not to say the avoided crossing revealed by the new model aren't important! These points may be utilized for Landau-Zener-Stückelburg transitions.

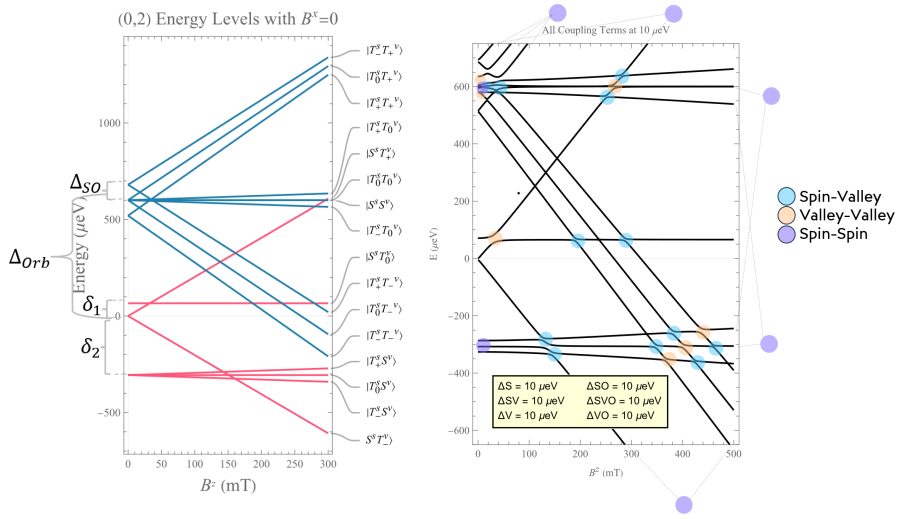

Figure 5: **Left:** Result of plotting only the diagonal elements of the H_2 matrix. This portion is well understood and the values used to make this plot were taken from [6,8]. The orbitally symmetric states are plotted in pink while the orbitally anti-symmetric states are plotted in blue. **Right:** Result of plotting the eigenvalues of H_2 with the flip coupling strength exaggerated for visibility. Each avoided crossing is marked with a color corresponding to the type of coupling which produced it.

Future Work

This work has been expanded to include a Hamiltonian for the (1,1) states and a tunneling Hamiltonian to describe the transition from the (1,1) to (0,2) states. The model developed over the course of this summer will be used to explain data from experiments probing the (1,1)→(0,2) transition and in planning Landau-Zener-St uckelburg transition tests. We hope to develop the first bilayer graphene qubit with the realization of a charge detector similar to

those used with semiconductor spin qubits. With a charge sensor actualized, BLG will be a substantial step closer toward use in quantum information experiments.

Acknowledgements

J.M. extends his sincerest gratitude toward the Global Quantum Leap program, and particularly to Steven Koester and Jordan Schwed, for organizing and supporting this one of a kind research experience. He would also like to acknowledge the Matter and Light for Quantum Computing cluster of excellence for the programming and support he received while in Germany. J.M. will be forever grateful for the hospitality, friendship, and guidance he received from the members of the 2nd Institute of Physics A at RWTH Aachen, and particularly from the BLG QD team!

References

[1] L. Banszerus, S. Möller, K. Hecker, E. Icking, K. Watanabe, T. Taniguchi, F. Hassler, C. Volk, and C. Stampfer. Particle–hole symmetry protects spin-valley blockade in graphene quantum dots. *Nature*, 618:51–56, 6 2023.

[2] L. Banszerus, A. Rothstein, T. Fabian, S. Möller, E. Icking, S. Trellenkamp, F. Lentz, D. Neumaier, K. Watanabe, T. Taniguchi, F. Libisch, C. Volk, and C. Stampfer. Electron–hole crossover in gate-controlled bilayer graphene quantum dots. *Nano Letters*, 20:7709–7715, 10 2020.

[3] Xinxin Cai, Elliot J. Connors, Lisa F. Edge, and John M. Nichol. Coherent spin–valley oscillations in silicon. *Nature Physics*, 19:386–393, 3 2023.

[4] Ryan M. Jock, N. Tobias Jacobson, Martin Rudolph, Daniel R. Ward, Malcolm S. Carroll, and Dwight R. Luhman. A silicon singlet–triplet qubit driven by spin-valley coupling. *Nature Communications*, 13, 12 2022.

[5] C. L. Kane and E. J. Mele. Quantum spin hall effect in graphene. *Physical Review Letters*, 95(22), November 2005.

[6] Angelika Knothe and Vladimir Fal'Ko. Quartet states in two-electron quantum dots in bilayer graphene. *Physical Review B*, 101, 2020.

[7] Angelika Knothe, Leonid I. Glazman, and Vladimir I. Fal'Ko. Tunneling theory for a bilayer graphene quantum dot's single- and two-electron states. *New Journal of Physics*, 24, 4 2022.

[8] S. Möller, L. Banszerus, A. Knothe, C. Steiner, E. Icking, S. Trellenkamp, F. Lentz, K. Watanabe, T. Taniguchi, L. I. Glazman, V. I. Fal'ko, C. Volk, and C. Stampfer. Probing two-electron multiplets in bilayer graphene quantum dots. *Physical Review Letters*, 127(25), December 2021.

[9] Takeshi Ota, Kenichi Hitachi, and Koji Muraki. Landau-zener-stückelberg interference in coherent charge oscillations of a one-electron double quantum dot. *Scientific Reports*, 8, 12 2018.

[10] Niklas Rohling and Guido Burkard. Universal quantum computing with spin and valley states. *New Journal of Physics*, 14(8):083008, August 2012.